Velocity model building by localized adaptive waveform inversion of early arrivals and reflections

P. Yong[1*], G. Provenzano[1], R. Brossier[1], L. Métivier[2,1],

[1]Univ. Grenoble Alpes, ISTerre, F-38058 Grenoble, France
[2]CNRS, Univ. Grenoble Alpes, LJK, F-38058 Grenoble, France

Friday 12th January, 2024

Main objectives

Improving the robustness and efficiency of waveform inversion for velocity macro-model building from limited-offset data.

New aspects covered

1. Concise formalism for the integration of localized adaptive waveform inversion (LAWI) and joint full-waveform inversion (JFWI).

2. Comparison of LAWI and graph-space optimal transport (GSOT) in the framework of both FWI and JFWI.

3. Synthetic tests suggest that integrating JFWI and LAWI brings about higher-fidelity velocity macro-model building.

Summary

Robust velocity model building from limited-offset data sets remains a challenging task. Joint full-waveform inversion (JFWI) uses both early arrivals and reflections to reconstruct shallow and deep macro-velocities. The recently developed localized adaptive waveform inversion provides an effective way to capture phase mismatch between observed and predicted data via a local matching filter. We propose using the phase mismatch estimated by the same local matching filter to define a robust misfit function in JFWI. Preliminary numerical examples confirm that integrating JFWI and LAWI can significantly improve the velocity macro-model building.

Velocity model building by localized adaptive waveform inversion of early arrivals and reflections

Introduction

Successful velocity reconstructions by full-waveform inversion (FWI, Tarantola, 1984) rely on long-offset and low-frequency data. For limited-offset data, FWI struggles to reconstruct the low wavenumber components of deep targets, due to the lack of wide illumination angles beyond the depth sampled by diving waves (Wu and Toksöz, 1987). To address this, Xu et al. (2012) propose a reflection full-waveform inversion (RWI), which exploits the low-wavenumber contribution from reflection wavepaths for better velocity macro-model building at depth. Joint full waveform inversion (JFWI, Zhou et al., 2015) utilizes both reflections and early arrivals to constrain the shallow and deep subsurface velocities.

Enhancing phase information in misfit design can reduce its non-linearity, leading to a more robust inversion result against inaccurate starting models. The use of graph-space optimal transport (GSOT, Métivier et al., 2019) misfit function in the framework of JFWI has been shown to significantly improve velocity macro-model reconstruction (Provenzano et al., 2023). Recently,Yong et al. (2023a,b) proposed a method to implicitly measure the instantaneous time-shift between compared data through a local matching filter, called localized adaptive waveform inversion (LAWI). Analysis and numerical studies suggest that it can further enhance phase information, compared to GSOT. In this work, we investigate the performance of integrating JFWI and LAWI for velocity model building using limited-offset data lacking low frequencies.

Joint full-waveform inversion of early arrivals and reflections

The JFWI misfit function is defined with separated early arrivals d_0^{obs} and reflections δd^{obs} (Zhou et al., 2015)

$$\mathbb{J}_{L^2} = \frac{1}{2}\|W_{d_0}(Ru_0 - d_0^{obs})\|^2 + \frac{1}{2}\|W_{\delta d}(R\delta u - \delta d^{obs})\|^2, \tag{1}$$

where W_{d_0} and $W_{\delta d}$ are the weight functions aimed at balancing the contributions of the transmission and scattering wavefield, and R extracts the calculated wavefield at the receivers position. The predicted transmission and scattering wavefields (u_0 and δu) are determined by

$$A(m_0)u_0 = s, \tag{2}$$

$$A(m_0+\delta m)(u_0+\delta u) = s, \tag{3}$$

where A denotes the wave-modeling operator, while m_0 and δm are the background and scattering parameters. The tomographic gradient for background velocity m_0 can be computed via

$$\frac{\partial \mathbb{J}_{L^2}}{\partial m_0} = \langle \lambda_1 | \frac{\partial A(m_0)}{\partial m_0} u_0 \rangle_T + \langle \lambda_2 | \frac{\partial A(m_0+\delta m)}{\partial m_0} (u_0+\delta u) \rangle_T, \tag{4}$$

where $\langle .,. \rangle_T$ denotes zero-lag cross-correlation over the time interval $[0,T]$ and λ_1, λ_2 are the adjoint wavefields solutions of

$$A^\dagger(m_0)\lambda_1 = \frac{\partial \mathbb{J}_{L^2}}{\partial \delta u} - \frac{\partial \mathbb{J}_{L^2}}{\partial u_0}, \tag{5}$$

$$A^\dagger(m_0+\delta m)\lambda_2 = -\frac{\partial \mathbb{J}_{L^2}}{\partial \delta u}. \tag{6}$$

Equation (4) ensures that the gradient of m_0 is composed by tomographic diving and reflection wavepaths via suppressing the first-order migration isochrones (Zhou et al., 2015). In JFWI, as well as in RWI, the scattering wavefield δu is generated by the perturbation model δm, whereas the background model m_0 needs remaining smooth. Such a scale-separation between a 'propagator' and a 'reflectivity' benefits from a [velocity (m_0) - impedance (δm)] parameterization, in virtue of non-overlapping virtual-source radiation patterns (Zhou et al., 2015).

The impedance perturbation δm (reflectivity) can be obtained by a least-squares migration (Nemeth

et al., 1999), whose convergence can be accelerated by employing a deconvolution imaging condition (Provenzano et al., 2023). Conventionally, δm and m_0 undergo an alternate update process. To reduce the need for repeated least-squares migrations and enforce consistency between velocity and reflectivity, JFWI can be reformulated in the pseudotime (vertical-traveltime) domain at no extra-cost, through an efficient 1D transformation (Plessix, 2013; Brossier et al., 2015; Provenzano et al., 2023).

Misfit function defined by localized adaptive waveform inversion

Given observed data $d(t)$ and predicted data $p(t)$ representing either early arrivals or reflections, the local matching filter used in LAWI is defined by a non-stationary convolution model in the time-frequency domain (Yong et al., 2023a):

$$\hat{w}(t,\omega)\hat{d}(t,\omega) = \hat{p}(t,\omega), \tag{7}$$

where $\hat{d}(t,\omega)$ and $\hat{p}(t,\omega)$ are the time-frequency spectra of observed and predicted data. The local matching filter can be computed with a delta-type regularization for Gabor deconvolution (Yong et al., 2023b). Applying inverse Fourier transform in τ domain, we obtain the local matching filter $w(t,\tau)$:

$$w(t,\tau) = \mathscr{F}_{\tau}^{-1}\left[\hat{w}(t,\omega)\right]. \tag{8}$$

The centroid time of the matching filter, representing instantaneous time shift between observed and predicted data, can be estimated by

$$T(t) = \frac{\int_{\mathbb{R}} |\tau| w^2(t,\tau)\mathrm{d}\tau}{\int_{\mathbb{R}} w^2(t,\tau)\mathrm{d}\tau}. \tag{9}$$

Integrating instantaneous time shift gives the objective function of LAWI. In the framework of JFWI, two independent local matching filters are designed for pre-separated early arrivals and reflections, and the objective function reads:

$$\mathbb{J}_{JLAWI} = \frac{1}{2}\int_{\mathbb{R}} T_{d_0}^2(t)\mathrm{d}t + \frac{1}{2}\int_{\mathbb{R}} T_{\delta d}^2(t)\mathrm{d}t. \tag{10}$$

Embedding LAWI into JFWI only requires modifying the adjoint sources in equations (5) and (6) to account for the misfit function change. It is noteworthy that LAWI prioritizes phase mismatch over amplitude mismatch, removing the need for non-trivial weight tuning between early arrivals and reflections.

2D Valhall example with limited-offset data

We test the performance of L^2-norm, GSOT and LAWI in the framework of both FWI and JFWI. A reflection streamer survey, consisting of 64 shots spaced 240 m apart and 228 receivers at 25 m spacing, is simulated on a 2D model inspired by a shallow-water exploration target (Fig. 1a). The model is defined on a 141×645 grid, with a spatial interval of 25 m. A 4 Hz Ricker wavelet, with energy below 1.5 Hz removed, is used to generate a 4.8 s observed data set. Notably, the limited-offset (< 6 km) poses significant challenges to waveform-based velocity reconstruction at the target depths, while the simple 1D starting velocity model exposes FWI to cycle-skipping (Fig. 1b). The true and initial density models are obtained via a Gardner's law. While the observed data is generated with a free-surface boundary condition, it is important pointing out that no de-ghosting or de-multiple are applied prior to inversion.

Figs 2 (a,c,e) display reconstructed velocity models using FWI. With the challenging setup, all the reconstructed models fail to obtain the true velocity trend, regardless of the misfit function employed. Quantitatively, this can be seen in the model misfit evolution of Fig. 3 (a), all reaching a high-valued plateau. L^2-norm FWI encounters line-search failure, stopping at the 22nd iteration. LAWI (Fig. 2e) seems to outperform the other misfit functions in delineating the low-velocity layers, while its velocity decrease is under-estimated due to the lack of deeply-reaching diving waves. This shows at the same time its potential, and the interest of combining it with JFWI. Thanks to its phase-driven nature, LAWI can balance the gradient contribution from early arrivals of large amplitude and deep reflections of weak amplitude, thus simultaneously updating both shallow and deep model. On the contrary, L^2 norm (Fig. 2a) and GSOT (Fig. 2c), more affected by amplitude discrepancies, privileged shallow model updates.

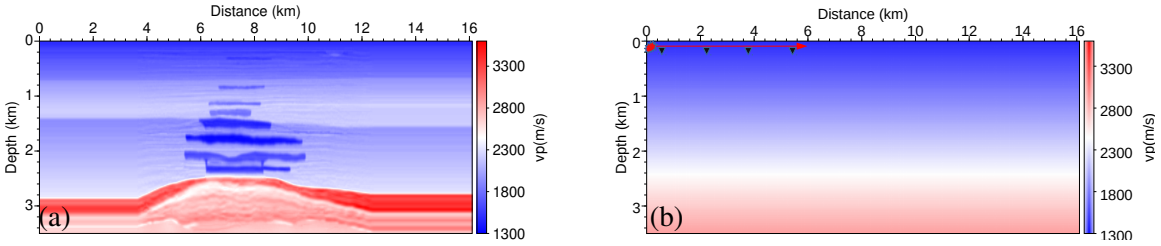

Figure 1 *True synthetic model: (a) P-wave velocity model, (b) 1D initial model. A surface streamer acquisition with maximum offset of 5960 m is used in the inversion.*

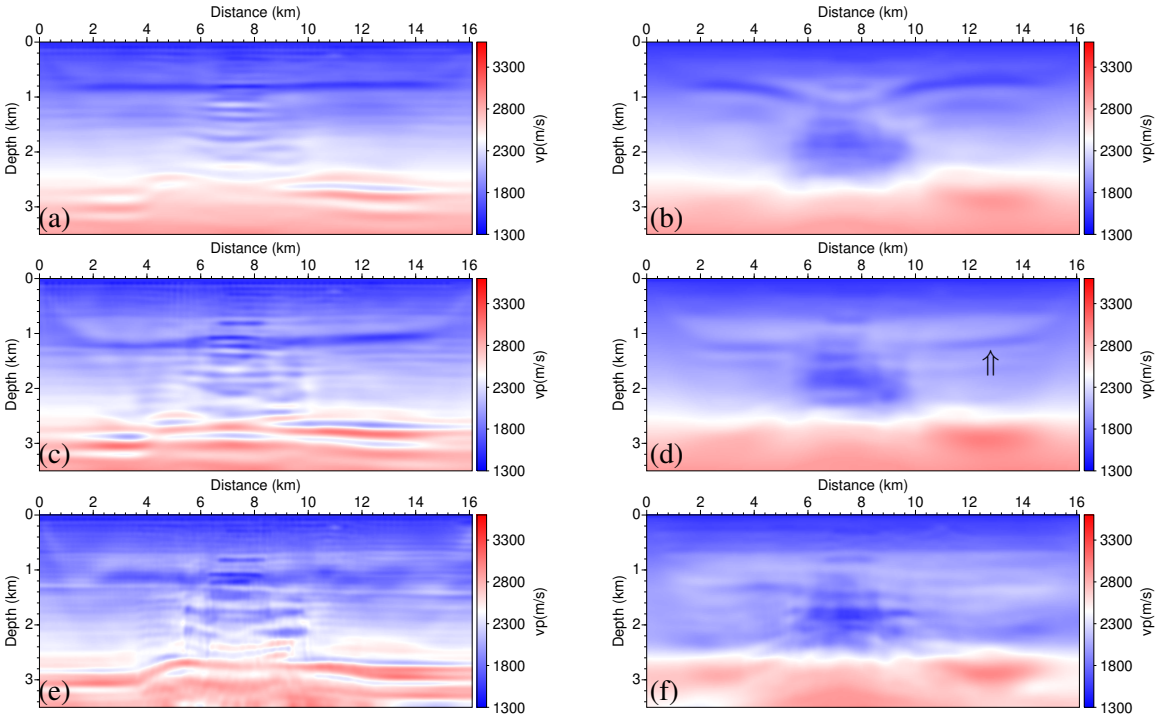

Figure 2 *Comparison of reconstructed velocity models by FWI (left-hand side) and JFWI (right-hand side) with different misfit functions: (a-b) L^2 norm, (c-d) GSOT, and (e-f) LAWI.*

Different from FWI that is capable of generating high-resolution velocity models, Figs 2 (b,d,f) show that JFWI primarily emphasizes background velocity updates. Comparison of these figures suggests that the misfit function plays a significant role in the framework of JFWI: The L^2-norm inversion (Fig. 2b) is trapped in an apparent local minimum, resulting in non-physical shallow updates. Although GSOT provides a more accurate velocity macro-model, it exhibits similar downward-bending low-velocity artifacts. The phase-driven LAWI can reduce the non-linearity of velocity inversion, and yields the most accurate velocity macro-model (Fig. 3b). It is worth noting that, while lacking high-wavenumber updates, the JFWI macro-models all exhibit a lower model misfit than the FWI ones. For a further comparison, we conducted subsequent GSOT-FWI and LAWI runs, initiating from their respective JFWI macro-models: The final results (Fig. 4) show that LAWI outperforms GSOT in dealing with cycle-skipping and in reconstructing broadband velocity models from limited-offset data that lacks low frequencies.

Conclusions

Conventional full-waveform inversion struggles to reconstruct background velocities beyond the penetration depth of diving waves. The JFWI framework jointly uses early arrivals and reflections to mitigate this limitation. The phase-driven LAWI misfit function can balance the contributions of early arrivals and reflections to the JFWI gradient, benefitting the simultaneous reconstruction of shallow and deep velocity trends. A 2D numerical study illustrates that combining JFWI and LAWI improves the reliability of velocity macro-model building in heavily cycle-skipped scenarios.

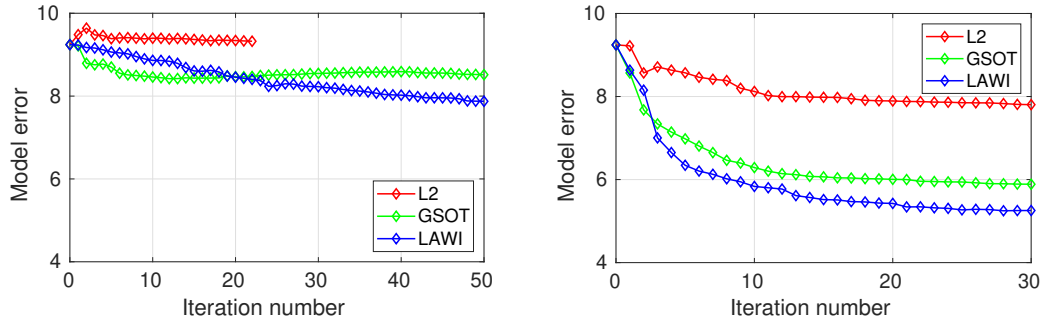

Figure 3 *Comparison of L^1-norm model error evolution with iterations: (a) FWI and (b) JFWI.*

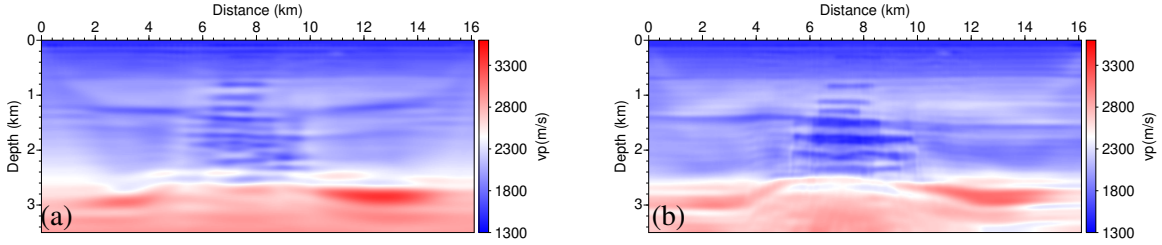

Figure 4 *Reconstructed velocity models by FWI starting from the JFWI results using the misfit functions of (a) GSOT and (b) LAWI.*

Acknowledgements

This study was partially funded by the SEISCOPE consortium (`http://seiscope2.osug.fr`), sponsored by AKER BP, CGG, DUG, EXXONMOBIL, GEOLINKS, JGI, PETROBRAS, SHELL, SINOPEC and TOTALENERGIES. This study was granted access to the HPC resources provided by the GRICAD infrastructure (https://gricad.univ-grenoble-alpes.fr), Cray Marketing Partner Network (`https://partners.cray.com`) and IDRIS/TGCC/CINES under the allocation 046091 made by GENCI.

References

Brossier, R., Operto, S. and Virieux, J. [2015] Velocity model building from seismic reflection data by full waveform inversion. *Geophysical Prospecting*, **63**, 354–367.

Métivier, L., Brossier, R., Mérigot, Q. and Oudet, E. [2019] A graph space optimal transport distance as a generalization of L^p distances: application to a seismic imaging inverse problem. *Inverse Problems*, **35**(8), 085001.

Nemeth, T., Wu, C. and Schuster, G.T. [1999] Least-squares migration of incomplete reflection data. *Geophysics*, **64**(1), 208–221.

Plessix, R.E. [2013] A pseudo-time formulation for acoustic full waveform inversion. *Geophysical Journal International*, **192**, 613–630.

Provenzano, G., Brossier, R. and Métivier, L. [2023] Robust and efficient waveform-based velocity-model-building by optimal-transport in the pseudotime domain: methodology. *Geophysics*, **88**(2), U49–U70.

Tarantola, A. [1984] Inversion of seismic reflection data in the acoustic approximation. *Geophysics*, **49**(8), 1259–1266.

Wu, R.S. and Toksöz, M.N. [1987] Diffraction tomography and multisource holography applied to seismic imaging. *Geophysics*, **52**, 11–25.

Xu, S., Wang, D., Chen, F., Lambaré, G. and Zhang, Y. [2012] Inversion on Reflected Seismic Wave. *SEG Technical Program Expanded Abstracts 2012*, 1–7.

Yong, P., Brossier, R., Métivier, L. and Virieux, J. [2023a] Localized adaptive waveform inversion: theory and numerical verification. *Geophysical Journal International*, **233**(2), 1055–1080.

Yong, P., Brossier, R., Métivier, L. and Virieux, J. [2023b] Localized adaptive waveform inversion: regularizations for Gabor deconvolution and 3D field data application. *Geophysical Journal International*, **235**(1), 448–467.

Zhou, W., Brossier, R., Operto, S. and Virieux, J. [2015] Full Waveform Inversion of Diving & Reflected Waves for Velocity Model Building with Impedance Inversion Based on Scale Separation. *Geophysical Journal International*, **202**(3), 1535–1554.